Effect of cascade transitions on the polarization of light emitted after electron-impact excitation of Zn by spin-polarized electrons

K. Bartschat, O. Zatsarinny, C. J. Bostock, D. V. Fursa, I. Bray, and A. N. Grum-Grzhimailo

The effect of cascade transitions on the polarization of light emitted after electron-impact excitation of Zn by spin-polarized electrons

K. Bartschat* and O. Zatsarinny

Department of Physics and Astronomy, Drake University, Des Moines, Iowa 50311, USA

C. J. Bostock, D. V. Fursa, and I. Bray

Curtin Institute for Computation and Department of Physics and Astronomy, Perth, 6102 Western Australia, Australia

A. N. Grum-Grzhimailo

Skobeltsyn Institute of Nuclear Physics, Lomonosov Moscow State University, Moscow 119991, Russia
(Dated: June 10, 2019)

We investigate the possible effect of cascade transitions from the $(4s5p)^3P_{0,1,2}$ states to the $(4s5s)^3S_1$ state of Zn. The polarization of the light emitted in the subsequent decay to the $(4s4p)^3P_{0,1,2}$ states has been the subject of recent controversy, with significant disagreement between the experimental data reported by Pravica et $al.$ (Phys. Rev. A **83** (2011) 040701) and by Clayburn and Gay (Phys. Rev. Lett. **119** (2017) 093401) in the cascade-free region below ≈ 7.6 eV incident energy and relatively good agreement above. The cross sections for excitation of the $(4s5p)^3P_{0,1,2}$ states, as well as higher-lying triplet states, and the linear polarization of the cascade radiation seem too small to produce a significant alignment of the $(4s5s)^3S_1$ state, thereby raising additional questions regarding the origin of the relatively large linear polarizations measured above the cascade threshold.

I. INTRODUCTION

In a recent paper, Clayburn and Gay [1] reported their measurements of the angle-integrated relative Stokes parameters (P_1, P_2, P_3) in the $(4s5s)^3S_1 \rightarrow (4s4p)^3P_0$ transition in Zn. These light polarizations completely characterize the polarization state of the emitted radiation. Specifically, with the light detector placed at right angle to the incident beam direction, P_1 and P_2 are the linear polarizations for $(0°, 90°)$ and $(45°, 135°)$ transmission, respectively, while P_3 is the circular polarization [2].

Of particular interest in this case is the linear polarization P_2. Clayburn and Gay found significant disagreement of their data with the measurements reported by Pravica et $al.$ [3] in the cascade-free region of incident electron energies below ≈ 7.6 eV, where the $(4s5s)^3S_1$ state can only be excited directly (no cascades) via an electron exchange transition. Being an S state that is classified to be essentially 100% pure [4], a spin polarization of the incident beam can be transferred to the excited Zn state and lead to circularly polarized radiation. A measurement of this circular polarization may, in fact, be used to optically determine the transversal spin polarization P_e of the incident beam [5], since P_3 is directly proportional to this parameter. A further consequence of this result is the fact that both P_1 and P_2 must vanish. By symmetry, P_2 is generally also proportional to P_e, but in this case the dynamics require the proportionality factor to vanish.

The above situation is a special case of a more general result derived a long time ago by Bartschat and Blum [6]:

If the excited state is purely LS-coupled, explicitly spin-dependent effects during the collision can be neglected, and there is no cascade population to account for, then P_2 should vanish. This prediction was confirmed in several experiments on heavy noble gases [7, 8] and held up well until the report by Pravica et $al.$ [3]. In a subsequent paper, Williams et $al.$ [9] proposed an explanation for their result. Their claim of a missing "geometrical phase" in the ab $initio$ quantum-mechanical numerical treatments drew several dissenting Comments [10, 11]. In one of those Comments [11], it was demonstrated that for a very heavy target such a Hg the total electronic angular momentum J in the $(6s7s)^3S_1$ state can indeed be aligned to a small extent, due to a combination of relativistic effects in the target description and some explicitly spin-dependent forces during the collision. However, even for Hg the magnitude of the near-threshold P_2/P_e value was far less than the $\approx 10\%$ found in Zn [3].

While the "zero" results of Clayburn and Gay for P_2/P_e below the cascade threshold in Zn, and hence the strong disagreement with the Pravica et $al.$ data in that energy region, may not be surprising in light of the states involved and the Bartschat-Blum theory, the two sets of experimental data agree (within the specified uncertainties) above the cascade threshold. Good agreement between the two experimental datasets also exists for both P_1 and P_3/P_e.

The principal motivation for the present study was the somewhat unexpected good agreement of P_2/P_e between the two sets of experimental data $above$ the cascade threshold, where significant nonzero values (about -10%) were reported from both experiments. This is particularly relevant a few eV above the excitation threshold. For the first 0.2 eV, only the $(4s5p)^3P_{0,1,2}$ states can be excited and subsequently emit radiation

---

*Electronic address: `klaus.bartschat@drake.edu`

that may populate and hence align the $(4s5s)^3S_1$ state. Given that these states are also well LS-coupled (about 95% [4]), one would not expect a significant polarization P_2/P_e either. The largest effect might come from the $(4s5p)^3P_1$ state, due to a small mixing with $(4s5p)^1P_1$, which violates the conditions outlined by Bartschat and Blum [6]. The $(4s5p)^3P_{0,2}$ states, on the other hand, should be nearly pure LS-states, and a $J = 0$ state cannot be aligned by any means. Consequently, one would expect P_2/P_e for $(4s5p)^3P_2 \rightarrow (4s5s)^3S_1$ to also be small.

While the $(4s4d)^3D_J$ states open up around 7.78 eV, followed by other states with configurations $(4s6s)$, $(4s6p)$, $(4s5d)$, and $(4s4f)$, the combined excitation cross sections of the triplet states from these configurations is relatively small (see Fig. 1 below). Furthermore, it seems highly unlikely that one- or multi-step cascades from these states to the $(4s5s)^3S_1$ state would collaborate in such a way that the latter state would become significantly polarized. Experience with cascades in general, in fact, suggests that depolarization effects would be the more probable outcome. Consequently, below we limit the treatment of cascade effects to those originating from the $(4s5p)^3P_J$ manifold. This is relatively straightforward and algebraically exact for the first 0.2 eV above threshold. It can also be expected to be very appropriate for the next few eV.

II. GENERAL THEORY

As shown in [6] and [13], all the light polarizations can be expressed in terms of so-called "angle-integrated state multipoles" (or "statistical tensors" [14]), which are a combination of the density-matrix elements describing an excited state. Specifically, only *relative* state multipoles enter, since everything can be normalized to the monopole $\langle \mathcal{T}(J)_{00}^+ \rangle$, which is proportional to the absolute cross section for excitation of the state with total electronic angular momentum J according to $\langle \mathcal{T}(J)_{00}^+ \rangle = Q(J)/\sqrt{2J+1}$.

A. Basic Formulas

We are specifically interested in electron impact excitation by a transversally spin-polarized electron beam without observation of the scattered electrons. Hence we define our coordinate system as follows: The z-axis is chosen along the incident-beam direction, while the spin-polarization defines the y-axis. This is also the direction along which the photon detector is placed. Due to the axial character of the spin-polarization vector, this problem has planar symmetry similar to an electron-photon coincidence setup with unpolarized electrons. However, additional restrictions apply. Specifically, Bartschat *et al.* [13] showed that the monopole $\langle \mathcal{T}(J)_{00}^+ \rangle$ as well as the alignment component $\langle \mathcal{T}(J)_{20}^+ \rangle$ are independent of the electron spin polarization, the state multipole $\langle \mathcal{T}(J)_{22}^+ \rangle$ vanishes, and $\langle \mathcal{T}(J)_{21}^+ \rangle$ as well as the orientation $\langle \mathcal{T}(J)_{11}^+ \rangle$ are directly proportional to the transversal spin polarization P_y. Furthermore, $\langle \mathcal{T}(J)_{21}^+ \rangle$ is real while $\langle \mathcal{T}(J)_{11}^+ \rangle$ is purely imaginary.

We now define the reduced state multipoles

$$\mathcal{A}_{kq}(J) = \langle \mathcal{T}(J)_{kq}^+ \rangle / \langle \mathcal{T}(J)_{00}^+ \rangle. \tag{1}$$

The second-rank multipoles ($k = 2$) describe the alignment of the angular momentum J, the first-rank multipoles ($k = 1$) describe its orientation. With these definitions, we can express the relative Stokes parameters for a transition to a final state with total electronic angular momentum J_f as

$$P_1 = -\frac{\alpha_2 \sqrt{3/8} \mathcal{A}_{20}(J)}{1 - \alpha_2 \mathcal{A}_{20}(J)/\sqrt{24}}, \tag{2a}$$

$$P_2 = \frac{\alpha_2 \mathcal{A}_{21}(J)}{1 - \alpha_2 \mathcal{A}_{20}(J)/\sqrt{24}}, \tag{2b}$$

$$P_3 = -\frac{\alpha_1 \text{Im}\{\mathcal{A}_{11}(J)\}}{1 - \alpha_2 \mathcal{A}_{20}(J)/\sqrt{24}}, \tag{2c}$$

where $\text{Im}\{X\}$ denotes the imaginary part of the quantity X and

$$\alpha_k = (-1)^{J+J_f+k+1} 3\sqrt{2J+1} \begin{Bmatrix} 1 & 1 & k \\ J & J & J_f \end{Bmatrix}. \tag{3}$$

Here $\begin{Bmatrix} j_1 & j_2 & j_3 \\ j_4 & j_5 & j_6 \end{Bmatrix}$ is a standard $6j$-symbol. For the $(4s5s)^3S_1 \rightarrow (4s4p)^3P_0$ transition we have $J = 1$ and $J_f = 0$. After evaluating the $6j$-symbols, this leads to $\alpha_k = \sqrt{3}$ for this case.

B. Inclusion of Cascades

We now consider cascades from an upper level with a total electronic angular momentum J_u down to a level with J. According to [15] (Section 3.4.2), the state multipoles "seen" experimentally (labelled by the superscript "e") are given by

$$\langle \mathcal{T}^e(J)_{kq}^+ \rangle = \langle \mathcal{T}(J)_{kq}^+ \rangle + \sum_{J_u} g(J, J_u, k) \langle \mathcal{T}^u(J_u)_{kq}^+ \rangle, \tag{4}$$

where the sum has to be performed over all upper levels that can cascade into the level of interest.

Equation (4) shows that *only* state multipoles of the same rank k and component q will contribute to a given state multipole of the state of interest, i.e., the state from which the radiation is ultimately observed. The factor $g(J, J_u, k)$ contains the relevant dipole matrix elements for the radiative transition, as well as several other terms that depend on the angular momenta of the various states involved. In principle, additional quantum numbers summarized by α_u and α could be introduced to

further specify the states of interest. However, we do not need them for the few states considered here and hence omit them for simplicity of notation.

In order to apply the above equations to our specific case, we now make a few important, though very appropriate assumptions. To begin with, we limit ourselves to cascade effects involving only the $(4s5p)^3P_{0,1,2}$ states. Note that these states practically decay only to the $(4s5s)^3S_1$ state. We therefore neglect the small decay probabilities from the $(4s5p)^3P_1$ state to both the $(4s5s)^1S_0$ excited state and the $(4s^2)^1S_0$ ground state, which can be nonzero due to the intermediate-coupling nature of the $(4s5p)^3P_1$ state. Based on our own structure calculations, as well as the very small relative intensity of the $(4s5p)^3P_1 \rightarrow (4s^2)^1S_0$ line and the absence of a $(4s5p)^3P_1 \rightarrow (4s5s)^1S_0$ line in the NIST Atomic Spectra database [4], we estimate the branching ratio to be less than 0.01%. Finally, we assume that the observed radiation from the $(4s5p)^3P_{0,1,2}$ states is coming from in-

coherently excited fine-structure levels. Note that there is no time resolution in the experiment under consideration. The above assumption is valid, since the line width of the emitted cascade radiation is much smaller than the fine-structure splitting of the energy levels.

With these assumptions the general expression (3.78) of [15] simplifies considerably, giving the factor $g(J, J_u, k)$ in Eq. (4) as

$$g(J, J_u, k) = (-1)^{J+J_u+k+1} (2J_u + 1) \begin{Bmatrix} J_u & J & 1 \\ J & J_u & k \end{Bmatrix}. \quad (5)$$

Note that all dipole matrix elements for the $(4s5p)^3P_{0,1,2} \rightarrow (4s5s)^3S_1$ transitions cancel as these radiative decay channels are either the only possible ones or at least by far dominant. Using the values $J = 1$ and $J_u = 0, 1, 2$ in Eq. (5) and collecting all the factors, we obtain

$$\langle \mathcal{T}^e(1)_{00}^+ \rangle = \langle \mathcal{T}(1)_{00}^+ \rangle + \left[\langle \mathcal{T}^u(0)_{00}^+ \rangle + \sqrt{3} \langle \mathcal{T}^u(1)_{00}^+ \rangle + \sqrt{5} \langle \mathcal{T}^u(2)_{00}^+ \rangle \right] / \sqrt{3}; \quad (6a)$$

$$\langle \mathcal{T}^e(1)_{11}^+ \rangle = \langle \mathcal{T}(1)_{11}^+ \rangle + \left[\langle \mathcal{T}^u(1)_{11}^+ \rangle + \sqrt{5} \langle \mathcal{T}^u(2)_{11}^+ \rangle \right] / 2; \quad (6b)$$

$$\langle \mathcal{T}^e(1)_{20}^+ \rangle = \langle \mathcal{T}(1)_{20}^+ \rangle - \left[\langle \mathcal{T}^u(1)_{20}^+ \rangle - \sqrt{7} \langle \mathcal{T}^u(2)_{20}^+ \rangle \right] / 2; \quad (6c)$$

$$\langle \mathcal{T}^e(1)_{21}^+ \rangle = \langle \mathcal{T}(1)_{21}^+ \rangle - \left[\langle \mathcal{T}^u(1)_{21}^+ \rangle - \sqrt{7} \langle \mathcal{T}^u(2)_{21}^+ \rangle \right] / 2. \quad (6d)$$

Equation (6a) expresses the fact that the apparent (i.e., observed) absolute cross section in this case is the sum of the direct cross section for the $(4s5s)^3S_1$ state plus the excitation cross sections for the $(4s5p)^3P_{0,1,2}$ states that decay into it.

As a final step, we use the state multipoles $\langle \mathcal{T}^e(1)_{kq}^+ \rangle$ to calculate the corresponding reduced state multipoles of Eqs. (1) and finally the light polarizations according to Eqs. (2).

III. COMPUTATIONS

In order to generate explicit values for the Stokes parameters, both characterizing the radiation from the directly excited $(4s5s)^3S_1$ and the $(4s5p)^3P_{0,1,2}$ states that can radiatively decay into the former state, we performed semi-relativistic Breit-Pauli collision calculations using the B-spline R-matrix (BP-BSR) method [16] and the associated computer code [17], as well as the fully relativistic convergent close-coupling (RCCC) approach [18, 19]. Specifically, the BP-BSR-43 model [20] coupled the lowest 29 discrete states of Zn up to $(3d^{10}4s4f)^1F_3$, together with the 14 states built from the configurations $(3d^{10}4p^2)$ and $(3d^94s^24p)$, respectively. The latter states lie above

the first ionization threshold of Zn and, to some extent, account for coupling to the ionization continuum. As a convergence check, we also carried out calculations with just the lowest 15 discrete levels (BP-BSR-15). As expected for the low projectile energies considered here, the results from the two models did not differ significantly to alter the conclusions drawn below.

The RCCC calculations were also performed in a variety of approximations. We again started by coupling just the lowest 15 discrete levels (the RCCC-15 model) before increasing the total number of states to 94. All states had an inert $3d^{10}$ Zn^{2+} core, but exchange with the inner electrons was included. The actual target states were then obtained by diagonalizing the quasi-two-electron Hamiltonian of the valence electrons in a large Laguerre basis. The Hamiltonian was supplemented by semi-empirical polarization potentials to account for the dipole polarizability of the doubly-ionized core. As in the BP-BSR case, the RCCC-15 predictions were very similar to the RCCC-94 results, which can safely be considered converged with the number of states included in the close-coupling expansion. For the physical states, the CCC structure results were similar to those of BP-BSR-43 published in [20] and are regarded as sufficiently accurate for the problem at hand. Occasionally, the collision re-

IV. RESULTS AND DISCUSSION

Figure 1 shows the *absolute* cross sections for electron-impact excitation of the $(4s5s)^3S_1$ and $(4s5p)^3P_{0,1,2}$ states in Zn from the $(4s^2)^1S_0$ ground state. The BP-BSR-43 calculations in particular were performed on a narrow energy grid, which reveals a large number of resonance features, the most important ones of which are also visible in the RCCC-94 predictions. As will be seen below, however, these are largely irrelevant for the light polarizations that are the principal focus of the present paper. We also note that the relative excitation strengths of the fine-structure levels of the $(4s5p)^3P_{0,1,2}$ manifold agree well with the expected statistical ratio, i.e., being proportional to $2J_u + 1$, and that the excitation cross section of the $(4s5s)^3S_1$ state is comparable to that of the combined $(4s5p)^3P$ manifold. The RCCC-94 predictions are generally larger than those obtained with BP-BSR-43. Since for these low energies the results are essentially converged with the number of states included in the close-coupling expansion, these differences are due to the different structure descriptions used in the two approaches. As will be seen below, the predictions for the *relative* light polarizations are far less sensitive to details in the target structure than the absolute cross sections.

Also shown in Fig. 1 is the sum of the excitation cross sections to higher-lying triplet states. The curve suggests that these states should have little effect altogether. Furthermore, as mentioned already, the most probable (small) effect of multiple cascades would be depolarization of the state under observation.

Figures 2 and 3 show our results for the light polarizations P_1, P_2/P_e, and P_3/P_e for the two cascade transitions $(4s5p)^3P_1 \rightarrow (4s5s)^3S_1$ and $(4s5p)^3P_2 \rightarrow$

sults at individual energy points can become very sensitive to tiny differences (e.g., in resonance positions or very close to a threshold), but the overall conclusions of the present work are not affected. In fact, the principal result, namely a nearly vanishing P_2/P_e is very stable against changes in the structure and collision models.

In order to obtain the angle-integrated state multipoles, we used two different methods. The energy- and angle-dependent scattering amplitudes can be constructed from the output of the BSR code by using Eq. (2) of Bartschat and Scott [21]. Since the BSR program yields energy- and angular-momentum dependent transition ($\boldsymbol{T}$) matrix elements, it is convenient to carry out the angular integration over the spherical harmonics analytically as suggested in [13], perform the sum over the unobserved spin components of the projectile, and then express the bilinear products of angle-integrated scattering amplitudes directly in term of the above $\boldsymbol{T}$-matrix elements. A general computer code for this task was published by Grum-Grzhimailo [22]. The RCCC program, on the other hand, evaluates angle-dependent scattering amplitudes. Hence we performed the integration over the polar angle numerically while the integration over the azimuthal angle is just a multiplication by 2π, which cancels out in all relative parameters. Having completely independent computer programs and ways to obtain the final light polarizations gives us further confidence in the results presented below.
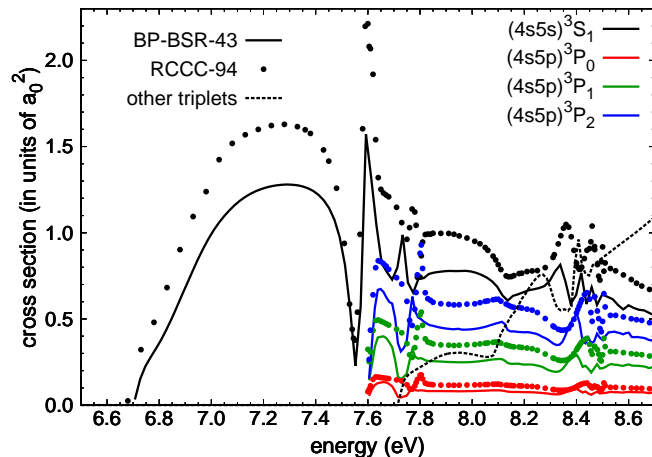

FIG. 1: Cross section for electron-impact excitation of the $(4s5s)^3S_1$ and $(4s5p)^3P_{0,1,2}$ states in Zn. The solid lines are the BP-BSR-43 results, while the small solid circles represent the RCCC-94 predictions. The dashed line represents the sum of the excitation cross sections to all the triplet states with configurations $(4s4d)$, $(4s6s)$, $(4s6p)$, $(4s5d)$, and $(4s4f)$, respectively, as obtained in the BP-BSR-43 model.
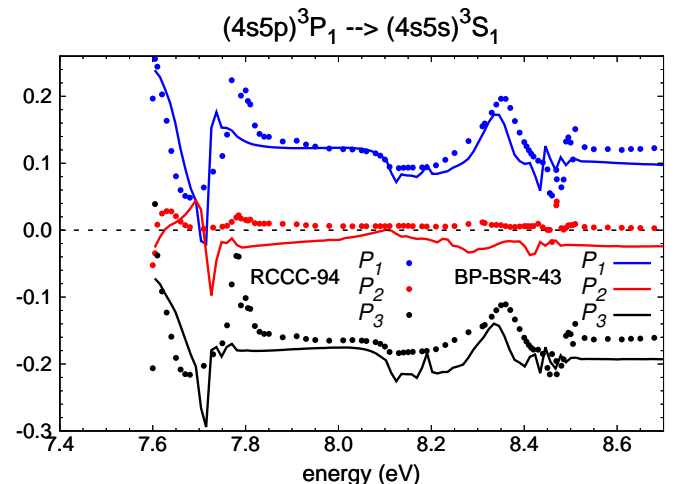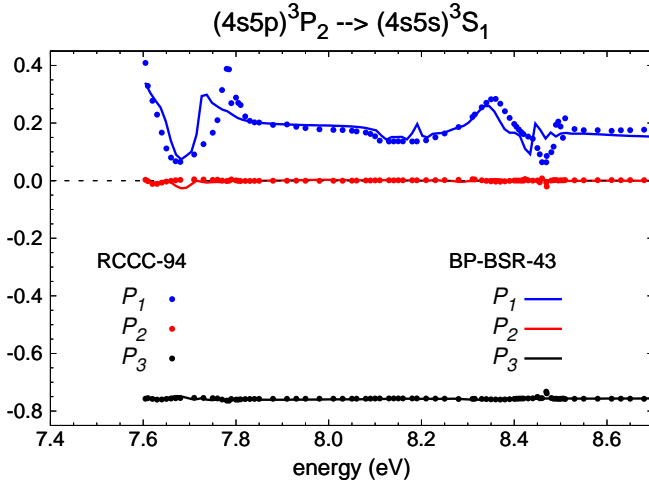

FIG. 2: Angle-integrated light polarizations for the $(4s5p)^3P_1 \rightarrow (4s5s)^3S_1$ transition. The solid lines are the BP-BSR-43 results, while the small solid circles represent the RCCC-94 predictions. P_1 is generally positive, P_3 is always negative, and $P_2 \approx 0$.

FIG. 3: Angle-integrated light polarizations for the $(4s5p)^3P_2 \rightarrow (4s5s)^3S_1$ transition. The solid lines are the BP-BSR-43 results, while the dashed lines the small solid circles represent the RCCC-94 predictions. P_1 is positive, $P_3 \approx -1$, and $P_2 \approx 0$.

$(4s5s)^3S_1$, respectively. Recall that all light polarizations for transitions starting at the $(4s5p)^3P_0$ state must vanish. Being P-states, their orbital angular momentum can be aligned, and hence it is not surprising that both of the above transitions show a significant nonzero linear polarization P_1, which also exhibits a substantial energy dependence. While the agreement between the BP-BSR-43 and RCCC-94 is by no means perfect for P_1, there is definitely good qualitative agreement. Very close to threshold (approximately $0-0.2$ eV above in our case), fractions like the light polarizations become very sensitive to details, both in the physics and the numerics, since both the numerator and the denominator approach zero at threshold. Furthermore, resonances that lead to different energy dependencies in the two parts of the fraction may have the largest effect. Hence, while the theoretical predictions are expected to be least reliable in this energy region, measurements would also be very difficult due to the anticipated small signal.

Moving on to the linear polarization P_2/P_e, we note that its magnitude is very small, except perhaps very close to the threshold in the $(4s5p)^3P_1$ state in the BP-BSR-43 results. Once again, this is not surprising at all. The $(4s5p)^3P_2$ state has virtually pure LS-character, and the $(4s5p)^1P_1$ admixture to the $(4s5p)^3P_1$ state is also very small. As mentioned above, we confirmed this by our own structure calculations, but the conclusion is also supported by the relative line strength of one and the absence of the other intercombination line in the NIST tables [4]. Hence, $P_2/P_e \approx 0$ is in excellent agreement with the Bartschat-Blum result [6]. We expect essentially zero for both cases. If there are deviations, they should be larger for the $(4s5p)^3P_1$ state than for the $(4s5p)^3P_2$ state due to the small intermediate-coupling character of the former state.

While it is extremely difficult to accurately calculate very small deviations from zero, we emphasize again that it is not essential for the conclusions of the present work whether P_2/P_e calculated here for just one of the cascade transitions (there are more for which the results are similar) is slightly positive or slightly negative. The important aspect is whether its magnitude reaches values that could ultimately lead to those reported in both experiments above the cascade threshold. Our present calculations, which represent the best we can do at this time, suggest that this is not the case.

Finally, the circular polarization P_3/P_e, once again, shows nonzero values for the $(4s5p)^3P_1 \rightarrow (4s5s)^3S_1$ transition with a clearly noticeable energy-dependence. Except very close to threshold, the agreement between the BP-BSR-43 and RCCC-94 predictions is very satisfactory. On the other hand, both theories yield a nearly energy-independent $P_3/P_e \approx -0.75$ for the $(4s5p)^3P_2 \rightarrow (4s5s)^3S_1$ transition. Since this came originally as a surprise to us, we carried out further analytical calculations along the lines of Bartschat and Blum [6] and Balashov et al. [15]. If one neglects the alignment term in the construction of $\langle \mathcal{T}(J)_{11}^+ \rangle$ according to Eq. (3) of [6], and also the alignment term in the denominator of Eq. (2c), one obtains

$$\langle \mathcal{T}(J=2)_{00}^+ \rangle = \frac{\sqrt{5/3}}{3} \langle \mathcal{T}(L=1)_{00}^+ \rangle; \quad (7a)$$

$$\langle \mathcal{T}(J=2)_{11}^+ \rangle = iP_e \frac{\sqrt{5/3}}{6} \langle \mathcal{T}(L=1)_{00}^+ \rangle; \quad (7b)$$

$$\mathrm{Im}\{\mathcal{A}_{11}(J)\} = P_e/2; \quad (7c)$$

$$P_3/P_e = -0.75. \quad (7d)$$

Equation (7a) is obtained by using the statistical factor $Q(J=2) = \frac{5}{9}Q(L=1)$, together with $\langle \mathcal{T}(J)_{00}^+ \rangle = Q(J)/\sqrt{2J+1}$ mentioned earlier and $\langle \mathcal{T}(L)_{00}^+ \rangle = Q(L)/\sqrt{2L+1}$. For a more general treatment, we refer to the Appendix.

Before we discuss our final results, it is worth summarizing the results for the cascade transitions. To begin with, we find that the $(4s5p)^3P_{0,1,2}$ states will essentially all decay to the $(4s5s)^3S_1$ state during an experiment that is performed in the way described above, i.e., without the observation of the scattered projectile and no resolution of the collision time. Since the $(4s5p)^3P_0$ state cannot be oriented or aligned at all, its (small) contribution to the observed light polarizations in transitions starting from the $(4s5s)^3S_1$ state will be a depolarization of the emitted radiation. The orbital alignment of the $(4s5p)^3P_{1,2}$ states leads to nonvanishing values of the linear polarization P_1, which can in turn align the M_J sublevels of the $(4s5s)^3S_1$ state and hence lead to an observable P_1 also for transitions from that state. Due to the very good LS-character of the $(4s5p)^3P_{0,1,2}$ states, however, the expected values for P_2/P_e remain close to zero, and hence the $(4s5s)^3S_1$ cannot be aligned in a way that a significant P_2/P_e would be seen in its subsequent optical decay. Finally, $|P_3/P_e|$ is less than unity, with a special

value of $P_3/P_e \approx -0.75$ for the $(4s5p)^3P_2 \to (4s5s)^3S_1$ transition. As a result, we expect a reduction in the spin orientation of the $(4s5s)^3S_1$ state and hence also a reduction of the observed circular polarization for incident energies above the cascade threshold. Finally, cascades from higher-lying states should have little effect due to the smallness of the respective excitation cross sections. Should there be a small effect, it will likely cause depolarization of the observed radiation.

In light of the above, our results shown in Fig. 4 for the three light polarizations in the $(4s5s)^3S_1 \to (4s4p)^3P_0$ transition are exactly what we expected. As for the cascade transitions, there is some noticeable structure in the energy dependence. This structure is due to resonances and increased sensitivity close to threshold, but we reemphasize that these details are not affecting the main message of this paper. Regarding P_1, the BP-BSR-43 and RCCC-94 predictions agree very well. Even though they are larger than the measured values (probably at least in part due to depolarization from cascades that we did not account for), there is definitely qualitative agreement with the experimental data from both groups, which also agree very well with each other. For P_2/P_e, we continue to predict essentially zero values. Our results agree with the measurements of Clayburn and Gay [1] below the cascade threshold, while their data above that threshold agree, within the error bars, with those of Pravica *et al.* [3]. Hence, both experimental datasets above the cascade threshold contradict general theory [6] as well as the present numerical calculations. Finally, there is excellent agreement between both theories and both experiments in the predicted depolarization of $P_3/P_e = -1$ below the cascade threshold when that threshold is crossed.

V. SUMMARY AND CONCLUSIONS

We have investigated the possible effect of cascade transitions from the $(4s5p)^3P_{0,1,2}$ states to the $(4s5s)^3S_1$ state of Zn. In our fully *ab initio* numerical calculations using a semi-relativistic 43-state Breit-Pauli B-spline R-matrix model and a fully relativistic 94-state close-coupling model, we obtained the cross sections for excitation of the $(4s5s)^3S_1$ and $(4s5p)^3P_{0,1,2}$ states, as well as the light polarizations for the cascade radiation $(4s5p)^3P_{1,2} \to (4s5s)^3S_1$ and, subsequently, for the $(4s5s)^3S_1 \to (4s4p)^3P_0$ transition observed experimentally. Accounting in an *ab initio* way for cascade effects shows that cascading only complicates the situation, but it does not change the underlying basic physics.

Our results are in excellent agreement with the general theoretical predictions made by Bartschat and Blum [6] many decades ago. Consequently, they also agree well with the P_2/P_e data of Clayburn and Gay [1] below the cascade threshold. However, our calculations raise new questions regarding, in particular, the relatively large magnitude of P_2/P_e reported in both experiments above the cascade threshold, where the agreement between the
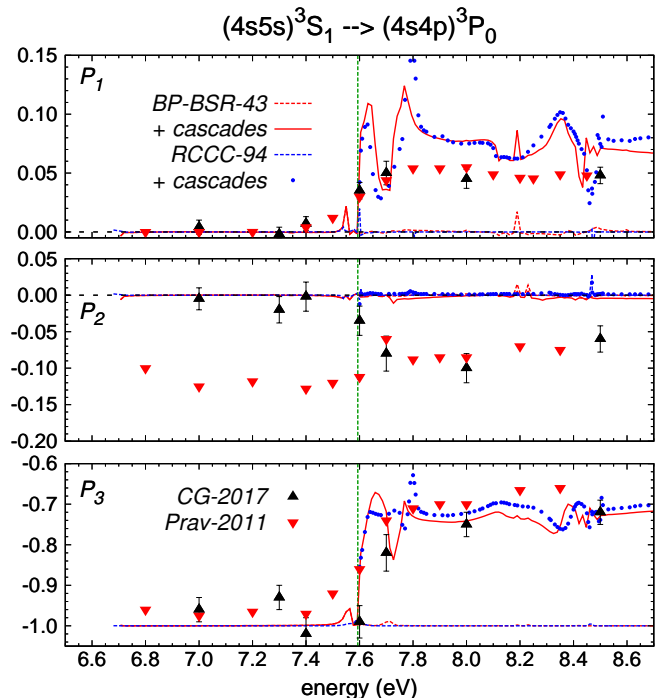

FIG. 4: Angle-integrated light polarizations for the $(4s5s)^3S_1 \to (4s4p)^3P_0$ transition. The dashed lines (almost indistinguishable from $P_1 = P_2/P_e = 0$ and $P_3/P_e = -1$) are the results without cascades, while the solid lines and small circles represent the BP-BSR-43 and RCCC-94, respectively, with the cascades included. The experimental data are: triangle-up: Clayburn and Gay [1]; triangle-down: Pravica *et al.* [3]. The published error bars on the latter are generally smaller than the symbol size.

experimental datasets, somewhat surprisingly, is very good. Additional experiments, with increased energy resolution and reduced uncertainties, seem highly desirable in order to resolve this issue. If our predictions were indeed incorrect, a shadow might be cast on essentially all collision calculations, at least for observables like those discussed in the present paper.

It may also be advisable to (re-)investigate other targets, in particular Hg. While some data exist for this case [11], we note that those were never published by the experimentalists themselves.

Acknowledgments

Appendix

This Appendix is devoted to the general derivation of angle-integrated state multipoles of an atomic state excited by a spin-polarized electron beam in the non-relativistic approximation. We start from the general Eq. (2.61) of [15], which describes (unnormalized) angle-differential state multipoles for the total angular momentum J of an atomic state excited by an arbitrarily polarized electron beam. Recall that we choose the z-axis along the incident electron beam, integrate analytically over the scattering angles, and sum over the unobserved spin components of the scattered projectile. Furthermore, we assume an atomic target initially in a closed-shell ($^1S_0$) configuration. Then we transform the scattering amplitudes from the jj-coupling scheme to the LSJ-coupling scheme, take into account conservation of the total spin S_t and the total orbital angular momentum L_t individually (i.e., $S_t = \frac{1}{2}$, and L_t equals the orbital momentum of the incoming electron, $L_t = \ell_0$). Many of the summations can then be performed analytically and the integrated reduced state multipoles can be expressed in terms of vector coupling coefficients and transition-matrix elements:

$$
\mathcal{A}_{kq}(J) = \frac{\left\langle T(J)^+_{kq} \right\rangle}{\left\langle T(J)^+_{00} \right\rangle} = (-1)^{k+L+S+1} 2\hat{J}\,\hat{L}^2\hat{S}^2 N^{-1}
$$

$$
\times \sum_{k_L k_s} \hat{k}_L \hat{k}_s (k_L 0, k_s q \mid kq) \left\{ \begin{matrix} \frac{1}{2} & \frac{1}{2} & k_s \\ S & S & \frac{1}{2} \end{matrix} \right\} \left\{ \begin{matrix} S & S & k_s \\ L & L & k_L \\ J & J & k \end{matrix} \right\} \rho_{k_s q}
$$

$$
\times \sum_{L_t L'_t \ell} (-1)^\ell (L_t 0, L'_t 0 \mid k_L 0) \left\{ \begin{matrix} L_t & L'_t & k_L \\ L & L & \ell \end{matrix} \right\} T_{L\ell L_t} T^*_{L\ell L'_t}, \quad (8)
$$

where

$$
N = \sum_{L_t \ell} \hat{L}_t^{-2} \{\ell L L_t\} \left| T_{L\ell L_t} \right|^2 . \quad (9)
$$

Here L and S are the total orbital angular momentum and spin of the excited atomic state, standard notations are used for the Clebsch-Gordan coefficients and the $6j$- and $9j$-symbols, $\hat{a} \equiv \sqrt{2a+1}$, $\{abc\} = 1$ if $a + b + c$ is integer and $|a - b| \leq c \leq a + b$, and $\{abc\} = 0$ otherwise. We also introduced a short-hand notation for the reduced transition-matrix elements

$$
T_{L\ell L_t} \equiv \langle (L, \ell)\, L_t \,\|\, T \,\|\, (0, \ell_0 = L_t)\, L_t \rangle, \quad (10)
$$

where T is a scalar operator in the subspace of the total orbital momentum, ℓ is the orbital angular momentum of the scattered electron, and $\boldsymbol{L} + \boldsymbol{\ell} = \boldsymbol{L}_t$. The statistical

tensors describing the spin of the incident electron $\rho_{k_s q}$ ($k_s = 0,\ 1$) are

$$
\rho_{00} = \frac{1}{\sqrt{2}}, \quad \rho_{10} = \frac{1}{\sqrt{2}} P_z, \quad \rho_{1\,\pm 1} = \mp \frac{1}{2}(P_x \mp iP_y). \quad (11)
$$

It follows from the $9j$-symbol with identical columns in Eq. (8) that $k_L + k_s + k$ must be even. Another observation is that the projection q in the integrated state multipole equals the projection of the electron tensor (11) and thus is restricted by $|q| \leq 1$. For this reason, for example, we did not consider the case $q = \pm 2$ in Eq. (6).

The incident electron beam in our derivation is still arbitrarily polarized and the x- and y-axes of the rectangular coordinate system need to be chosen. As in the main part of the manuscript, we take the y-axis along the transversal electron polarization, i.e., $P_x = P_z = 0$ and $P_y = P_e$. It is practical to split Eq. (8) into two parts corresponding to $k_s = 0$ (contribution from unpolarized electrons) and $k_s = 1$ (contribution from the electron beam polarization):

$$
\mathcal{A}_{kq}(J) = N^{-1}\hat{J} \Bigg[\delta_{q0}(-1)^{J+S} \hat{L}^2 \left\{ \begin{matrix} J & J & k \\ L & L & S \end{matrix} \right\}
$$

$$
\times \sum_{L_t L'_t \ell} (-1)^\ell (L_t 0, L'_t 0 \mid k0) \left\{ \begin{matrix} L_t & L'_t & k \\ L & L & \ell \end{matrix} \right\} T_{L\ell L_t} T^*_{L\ell L'_t}
$$

$$
+ \; iP_y \sqrt{3}\hat{L}^2 \hat{S}^2 (-1)^{k+L+S+1}
$$

$$
\times \sum_{k_L = k\pm 1} \hat{k}_L (k_L 0, 1q \mid kq) \left\{ \begin{matrix} \frac{1}{2} & \frac{1}{2} & 1 \\ S & S & \frac{1}{2} \end{matrix} \right\} \left\{ \begin{matrix} S & S & 1 \\ L & L & k_L \\ J & J & k \end{matrix} \right\}
$$

$$
\times \sum_{L_t L'_t \ell} (-1)^\ell (L_t 0, L'_t 0 \mid k_L 0) \left\{ \begin{matrix} L_t & L'_t & k_L \\ L & L & \ell \end{matrix} \right\}
$$

$$
\times \; T_{L\ell L_t} T^*_{L\ell L'_t} \Bigg]. \quad (12)
$$

With these reduced state multipoles we can find the Stokes parameters of the fluorescence radiation according to Eqs. (2a)-(2c).

Let us consider a few special cases of Eq. (12). For example, for singlet states ($S = 0, J = L$) only reduced statistical tensors with zero projection, $q = 0$, survive and form the first term of (12), $\mathcal{A}_{11}(J) = 0$, and therefore $P_3 = 0$. For S-states ($L = 0, J = S$) the result is independent of the scattering amplitudes:

$$
\mathcal{A}_{kq}(J) = \delta_{k0} + \delta_{k1} iP_y (-1)^J \sqrt{3} \left\{ \begin{matrix} \frac{1}{2} & \frac{1}{2} & 1 \\ J & J & \frac{1}{2} \end{matrix} \right\}. \quad (13)
$$

Since only $k = 0$ and $k = 1$ contribute in Eq. (13), $P_1 = P_2 = 0$. For the fluorescence transition $^3S_1 \to\, ^3P_0$, we obtain $P_3 = -P_y$, in excellent agreement with the cascade-free calculations shown in Fig. 4.

Finally, after substituting the quantum numbers for the $^3P_2$ state ($L = 1,\ S = 1,\ J = 2$) in Eq. (12), we

obtain

$$\mathcal{A}_{11}(^3P_2) = iP_y \left[\frac{1}{2} + \frac{\sqrt{3}}{10\sqrt{2}} N^{-1} \sum_{L_t L'_t \ell} (-1)^\ell (L_t 0, L'_t 0 \,|\, 20) \right.$$
$$\left. \times \begin{Bmatrix} L_t & L'_t & 2 \\ L & L & \ell \end{Bmatrix} T_{L\ell L_t} T^*_{L\ell L'_t} \right] . (14)$$

Assuming that the second term is much smaller than the

first because of a small algebraic coefficient and mutual cancellations of the interfering terms in the sum, we have $\mathcal{A}_{11}(^3P_2) = \frac{i}{2}P_e$. As mentioned in the main text, after also neglecting the alignment contribution in the denominator of (2c), we obtain $P_3/P_e = -\frac{3}{4}$ for the $^3P_2 \to {}^3S_1$ fluorescence radiation.

[1] N. B. Clayburn and T. J. Gay Phys. Rev. Lett. **119** (2017) 093401.

[2] N. Andersen and K. Bartschat, *Polarization, Alignment, and Orientation in Atomic Collisions* (2nd edition, Springer, New York, 2017)

[3] L. Pravica, J. F. Williams, D. Cvejanović, S. Samarin, K. Bartschat, O. Zatsarinny, A. D. Stauffer, and R. Srivastava, Phys. Rev. A **83** (2011) 040701(R).

[4] http://physics.nist.gov/cgi-bin/AtData.

[5] M. Eminyan and G. Lampel, Phys. Rev. Lett. **45** (1980) 1171.

[6] K. Bartschat and K. Blum, Z. Phys. A **304** (1982) 85.

[7] J. E. Furst, T. J. Gay, W. M. K. P. Wijayaratna, K. Bartschat, H. Geesmann, M. A. Khakoo, and D. H. Madison, J. Phys. B **25** (1992) 1089.

[8] J.E. Furst, W.M.K.P. Wijayaratna, D.H. Madison, and T.J. Gay, Phys. Rev. A **47** (1993) 3775.

[9] J. F. Williams, L. Pravica, and S. N. Samarin, Phys. Rev. A **85** (2012) 022701.

[10] C. J. Bostock, D. V. Fursa, and I. Bray, Phys. Rev. A **87** (2013) 016701.

[11] K. Bartschat and O. Zatsarinny, Phys. Rev. A **87** (2013) 016702.

[12] K. Blum, *Density Matrix Theory and Applications* (3rd edition, Springer, New York, 2012)

[13] K. Bartschat, K. Blum, G. F. Hanne, and J. Kessler, J. Phys. B **14** (1981) 3761.

[14] S. Devons and L. J. B. Goldfarb, *Angular Correlations*, in *Handbuch der Physik*, ed. S. Flügge, (Springer-Verlag, Berlin, 1957) **42** 362

[15] V. V. Balashov, A. N. Grum-Grzhimailo, and N. M. Kabachnik, *Polarization and Correlation Phenomena in Atomic Collisions: A Practical Theory Course* (Kluwer Academic / Plenum Publishers, New York, 2000).

[16] O. Zatsarinny and K. Bartschat, J. Phys. B **46** (2013) 112001.

[17] O. Zatsarinny, Comp. Phys. Commun. **174** (2006) 273.

[18] D. V. Fursa and I. Bray, Phys. Rev. Lett. **100** (2008) 113201.

[19] C. J. Bostock, D. V. Fursa, and I. Bray, Phys. Rev. A **82** (2010) 022713.

[20] O. Zatsarinny and K. Bartschat, Phys. Rev. A **71** (2005) 022716.

[21] K. Bartschat and N. S. Scott, Comp. Phys. Commun. **30** (1983) 369.

[22] A. N. Grum-Grzhimailo, Comp. Phys. Commun. **152** (2003) 101.